Air Bearing Force Measurement of Pico Negative Pressure Sliders during Dynamic Unload

M. Chapin and D. B. Bogy

Computer Mechanics Laboratory

Department of Mechanical Engineering

University of California

Berkeley, CA 94720

ABSTRACT

The air bearing forces of "pico negative pressure" (1.25x1.0 mm subambient pressure) sliders during the unload process were investigated experimentally. A high speed vertical load/unload mechanism with a sensitive force transducer was developed to measure the air bearing forces. Force histories were measured at various disk rpm and unload velocities. The force histories showed that the suspension load dimple separated from the load beam during the lifting. This separation was held to an acceptable amount by flexure limitors built into the suspension. Force-displacement curves show the need for control of the gap between the limitor and load beam. A technique was developed to determine critical suspension parameters for use in the CML Dynamic Load/Unload Simulator. Simulation of the force history was then in excellent agreement with experimental results. Both simulation and experimental results showed the lift-off force decreases with increasing disk rpm. Experimental results also showed that higher unload

speeds lead to larger lift-off forces. By selecting the correct disk rpm and unload speed, the lift-off force could be minimized.

I.   INTRODUCTION

The need for a more reliable head-disk interface and lower glide heights has been fueled by the need for ever increasing data storage capacity. The conventional contact-start-stop (CSS) disk drive has difficulties meeting the requirements of improved head-disk interface reliability and lower glide heights, using laser textured landing zones. As glide heights decrease further, the use of such textured zones will become even more difficult. Dynamic load/unload (L/UL) has been successfully implemented in portable disk drives to overcome these and other problems. The dynamic L/UL mechanism allows for increased head-disk reliability and eliminates the stiction problems of CSS, since the slider never lands on the disk during non-operating conditions. This in turn allows for smoother disks and thus lower glide heights. Some other advantages of dynamic L/UL include less power consumption and better non-operating shock resistance. The use of dynamic L/UL also frees up the laser textured landing zone so that data can now be written there. For these reasons, dynamic L/UL disk drives are becoming more popular in the industry.

There have been many studies on dynamic L/UL that investigated the loading process of positive pressure sliders. Jeong and Bogy [1-2] used experiment and simulation to show that head-disk contact during loading could be avoided if certain loading parameters were

realized. Such parameters included pitch static attitude, roll static attitude, and vertical

load velocity. Fu and Bogy [3-4] also studied the load process of positive pressure sliders

experimentally. Since the unload process of positive pressure sliders was less interesting,

it was not investigated. Until recently, little research has be done on the unload process

of negative pressure sliders. Hu et al [5], performed a numerical simulation of the unload

process for negative pressure sliders through a process known as "degramming." Peng

[6] showed through simulation that the ABS of negative pressure sliders generates a net

suction force during unload. Zeng et al. [7], showed a strong dependence of lift-off force

on disk rpm and unload speed in simulation results. The lift-off force was defined as the

maximum force needed to unload a slider. They also developed an experiment to

measure the air bearing forces during low speed L/UL of nano (2.0x1.6 mm) type sliders.

The experimental results confirmed the predicted dependence of lift-off force on disk

rpm. Due to the lack of an adequate high-speed vertical unload mechanism the

dependence of unload speed was not shown experimentally.

In this study, we investigated the dynamics of pico negative pressure sliders during the

unload process. The present goal of this study was to experimentally show the

dependence of lift-off force on both disk rpm and unload speed. To achieve high speed

unload, we built a new vertical L/UL mechanism. Due to the small forces associated

with the air bearing of pico type sliders, a new, more sensitive force transducer was also

built. Experiments showed that minimization of the lift-off force can be achieved by

selecting a high disk rpm and low unload velocity. We also investigated the unload air

bearing force history using head-gimble assemblies (HGA's) with special flexure

limitors. The suction forces result in the separation of the dimple from the load beam.

This separation is reduced due to the flexure limitors, which can be seen as a third stage

in the unload force histories. Necessary suspension parameters for use in the CML

Dynamic L/UL software were determined from the measured force histories. Finally,

simulations were carried out to compare the simulation and experimental results.

II.   EXPERIMENT APPARATUS

A. *Load/unload Mechanism*

As stated in the introduction, simulation data showed a strong dependence of lift-off force

on unload speed. In order to achieve higher L/UL speeds a new L/UL mechanism was

designed and built. Like the first generation L/UL mechanism [7], this mechanism was

designed for vertical loading and unloading. This was necessary because of the

difficulties associated with measuring slider dynamics and air bearing forces while

actuating the slider in the radial direction. In an attempt to emulate actual dynamic L/UL

disk drives under controlled L/UL, we designed the mechanism to actuate the slider at

constant vertical velocity. This proved to be a difficult task. In an actual L/UL disk drive

constant vertical velocity is achieved by a constant angular velocity of the voice coil

motor and a constant angle ramp along which the suspension slides. There is ample

radial distance to accelerate the head stack assembly to a high velocity. In a vertical

L/UL mechanism, there is very little vertical distance to accelerate the actuator to a high

velocity. This distance is simply the clearance between the disk and the L/UL tab, which

is usually less than 0.5 mm. To complicate matters further, there has to be some sort of lift coupling between the disk and L/UL tab, which decreases the distance for acceleration even more.

A dynamical analysis of various components of a vertical L/UL mechanism showed that the largest inertial mass was that of the L/UL mechanism's driving motor. Therefore, the key in attaining a high constant velocity in a negligible actuator displacement was to accelerate the motor to constant velocity while the vertical L/UL mechanism remained stationary. This was done through the use a cam and follower device. A schematic of the high speed L/UL mechanism is shown in figure 1. A profile of the cam used in the mechanism is shown in figure 2. Three regions can be seen in this profile. In the first region, the cam radius remains constant allowing the cam and motor to accelerate to the desired speed. The cam follower and vertical L/UL displacement remain unchanged. In the second region, the radius of the cam increases 1 mm linearly. In this stage, the cam achieves a constant velocity and executes the L/UL motion. Like the first stage, the third stage is used to decelerate the cam and motor to zero velocity while the vertical L/UL displacement remains stationary. The control of the L/UL mechanism's motor was also crucial for constant L/UL velocity. This was solved by using a computer-controlled servomotor. The system was able to achieve a constant vertical velocity of 10-15 mm/sec.

B. Force Transducer

To allow for accurate measurement of the small air bearing forces of a pico slider, we built a very sensitive force transducer. A simple aluminum cantilever affixed with strain gages was chosen as the transducer. Figure 1 also shows the force transducer with a head-gimble assembly (HGA) in the test position. The HGA lift tab, which is located at the slider end of the suspension, fits in the wire coupling which is rigidly attached to the end of the cantilever. During a L/UL cycle, forces generated at the air bearing are transferred to the cantilever through the lift tab.

A trade off between sensitivity and stiffness exists in a cantilever force transducer. For high-speed L/UL applications, it is necessary for the force transducer to respond quickly to variations in force, since the time for the unload process is usually less than 20 ms. This was achieved by increasing the cantilevers natural frequency or, likewise, its stiffness, which, in turn, decreased the transducer's sensitivity. It was found that a sensitivity of <10 grams/volt and a fundamental frequency of >4 kHz was satisfactory. A program was written to find the optimal dimensions of the cantilever. A full bridge of semiconductor strain gages was used to increase the transducer sensitivity. Finally, the output of the bridge was amplified with a Calex Model 165 Bridgesensor.

Two calibration methods were developed to convert voltage data into force data. Two forces were of interest during dynamic L/UL, that of the air bearing and that on the ramp. Figure 3 shows a schematic of the two calibration methods. In the first method, weights from 1 to 5 grams were hung from the backside of the load dimple. This gave a

calibration coefficient for the air bearing forces. In the second method, weights were hung directly from the lift coupling. This gave a calibration for the ramp forces. All data presented in this report used the first calibration method. The calibration coefficient was 8.06 grams/volt for this method. The cantilever's fundamental frequency was 4.25 kHz.

III. EXPERIMENTAL METHOD

Two identical pico negative pressure sliders mounted on suspensions designed specifically for L/UL were used in this study. The suspensions had two limitors to constrain the deflection of the flexure. The slider ABS design is shown in figure 4. The force data was amplified and then stored in a Lecroy 9304c digital oscilloscope. Force histories were captured at twelve different disk rpm's and two different unload velocities, which ranged from 2500 rpm to 10,000 rpm and .5 mm\sec to 11.25 mm\sec, respectively. All unload experiments were done at a disk radius of 45 mm and a +16° slider skew angle. At each of the experimental conditions, 50 unload force histories were averaged. This was done to increase the signal to noise ratio. It was found that disks and spindle motors with large vertical run out caused large oscillations in the force histories at low unload velocities. These were reduced by using a low run out air bearing spindle mounted on a TTI TriboCop spinstand. However, this did not eliminate the run out completely, since there was still run out associated with disk warpage.

In order to average many force histories, it was necessary to have a repeatable trigger signal to acquire the data. This trigger signal was generated by an LDV, which sensed

the sudden release of the slider from the disk. This trigger proved to be very repeatable.

We also did not want the averaging process to cancel out the disk run out generated

oscillations in the force, so it was necessary to start and end the unload process at the

same circumferencial point on the disk. This ensured that the force oscillations would

always be in phase and not cancel each other during averaging. The computer controlled

unload mechanism was used to solve this problem. The spindle index was used to trigger

the servo motor controller.

Finally, the averaged force data was processed further. This force data contained two

superimposed components, the air bearing force and the linearly increasing force

associated with the load beam stiffness. In order to measure the forces at the air bearing,

the load beam force needed to be subtracted out of the raw force data. Figure 5 shows a

typical raw force history curve. The last portion of the data represents the linearly

increasing force of the load beam. In this region, the slider had already released from the

disk while the unload mechanism was still lifting the suspension. A linear regression was

applied to this region, and then it was subtracted from the raw data to give the net air

bearing force.

IV. RESULTS

A. *Experimental Results*

The processed unload force history for a disk speed of 3,000 rpm and an unload speed of 11.25 mm/sec is shown in figure 6. For suspensions with flexure limitors, three distinct regions are seen. The first slope, which decreases from the initial 3.5 gram load to zero load, was the "degramming" [5] portion of the unload cycle. The first discontinuity, at zero force, is characterized by the separation of the dimple from the load beam. The first discontinuity is also seen in suspensions without flexure limitors if they still have a two piece design [7]. Once the dimple separates from the load beam, the stiffness of the system decreases dramatically due to the low stiffness of the flexure. In this region, it takes a relatively long time, and similarly a large unload displacement, for the negative force to build up. Once the force reached about –0.4 grams the limitors contacted the load beam. Again, this is seen in figure 6 as a discontinuity, or change in slope. The limitors tended to stiffen the system, which caused the negative force to build up much faster. The slider released from the disk when the force reached a critical value known as the lift-off force.

The lift-off force, as defined in the introduction, is simply the maximum net negative force at the air bearing before the slider releases from the disk. These values were read off the force histories at the various experimental conditions. These values are shown in

figure 7. Both samples were run three times at each of the experimental conditions, each

being an average of 50 unload cycles. The plotted data points are the average of the two

samples. The error bars represent $\pm 3\sigma$ standard deviations about the mean. From this

figure, two distinct trends can be seen. First, as the disk rpm increases, the magnitude of

the lift-off force decreases. This is seen at both unload speeds. Second, larger lift-off

forces are generated by higher unload speeds. It should be noted that the actual

dependence of lift-off force on disk rpm varies with HGA design [6,7].

B. Suspension and ABS Parameter Determination

The CML Dynamic L/UL simulation software [8] was used to simulate the unload

process for this particular ABS design and suspension. The simulator requires the user to

input the ABS geometry and certain suspension parameters. The ABS geometry was

measured with a toolmakers microscope equipped with pattern recognition software. The

cavity depths were measured with a Dektak surface profiler. For each of the regions, the

suspension parameters required for the simulation were as follows: the system stiffness in

that region, the forces which define the boundaries of that region, and a parameter called

X_d. The parameter X_d specifies the offset in the length direction from the slider center

where the lifting force acts.

It is possible to obtain all the necessary suspension parameters with a well-posed FE

model. However, if a FE model is not available, one can determine these parameters

experimentally with a force-displacement curve. The force-displacement curve of figure

6 is shown again in figure 9, but the time axis in figure 6 has been multiplied by the unload velocity to obtain a force-displacement curve. The stiffness values were obtained from this plot by fitting lines to the three regions. The forces at the boundaries of each region were also read off this plot. The calculated stiffness for region 1 is 981 N/m with force boundaries of 3.5 grams and 0 grams. The stiffness values for regions 2 and 3 are 34.4 N/m and 265 N/m, respectively. The force boundary between region 2 and 3 is -0.405 grams. It is not necessary to specify the force at the end of region 3, this was the lift-off force. The parameter X_d significantly affects the lift-off force predicted by the simulation. Simulations were run at 3000 rpm and an unload speed of 11.25 mm/sec while varying X_d. The actual values of X_d were determined by having the simulated lift-off force match that of the experiment. The following are the values for X_d: X_d 1 = 0.0 mm, X_d 2 = -0.2 mm, and X_d 3 = -0.09 mm. Negative values represent offsets toward the leading edge of the slider. These values were held constant throughout all simulation runs.

C. Simulation Results

The simulated force history for the above suspension parameters at 3000 rpm with an unload speed of 11.25 mm/sec is shown in figure 9. A comparison of the experimental and simulated force histories shows excellent agreement. The maximum lift-off force for the experimental case is –0.89 grams while the simulated case is –0.87 grams. Simulations were also conducted at four different disk speeds; 3000 rpm, 54000 rpm, 7200 rpm and 10000 rpm, all at an unload speed of 11.25 mm/sec. The lift-off force was

determined from the force histories and plotted as the dashed line in figure 7. Again, one can see excellent correlation between experiment and simulation.

One might be skeptical of the correlation between experiment and simulation because of the method employed to determine the suspension parameters, such as X_d. This parameter was varied iteratively until the simulation matched the experiment. This guaranteed a very precise match between experiment and simulation only at 3000 rpm. The true test of how well these suspension parameters predicted the experimental lift-off force was at the other three disk speeds. Since the suspension parameters predicted the lift-off force accurately at the other disk speeds, it is concluded that the parameters were indeed accurate.

V. DISCUSSION

The force histories give many interesting insights into the unload process.   First and foremost, it gives the lift-off force for a certain HGA design. This value is crucial in the design of the suspension. Suspension stiffness will be determined by this value as will the limitor gap. Soft suspensions take a long time and large distance to unload. With a ramp angle of 15 degrees, the radial displacement of the slider is 4 times greater than the displacement in the vertical direction. Since the data zone must end before the HGA contacts the ramp, soft suspensions will lead to a lose of valuable recording area on the disk. With decreasing drive heights, there is also a concern that the vertical lift displacements will interfere with the single-disk half space [9]. The limitor gap must also

be controlled precisely. A large limitor gap allows the unload cycle to stay in the second stage for a larger time where the systems stiffness is the smallest. Again, this would lead to larger spacing between the disks and a loss of recording area on the disk.

The choices of unload velocities and disk speeds are crucial for unload. As seen in figure 7, there is a strong dependence of lift-off force on disk speed and unload velocity. There are two reasons to minimize the lift-off force during unload. First is the issue of recording area loss. A slider unloads from the disk with less vertical and radial displacement if the lift-off force is decreased. Second, there is a possibility of catastrophic head-disk contact during unload. This could occur if the lift-off force is so large that the slider rebounds off the load beam and hits the disk. During a system power failure, the unload motion may be uncontrolled. In this case very little can be done to choose the correct unload velocity and disk speed. Special ABS designs that do not create significant lifting force must be considered to solve this problem [7].

Various hypotheses have been postulated to explain the trends seen in figure 7. It is thought that the dependence of lift-off force on disk speed is an issue related to flying pitch. As the disk speed increases, the flying pitch also increases provided there is substantial rail area at the leading edge. Since there is an increased pitch, the slider will tend to "peel" off the disk. This "peeling" effect tends to reduce the lift-off force. As indicated by the negative X_d values in the last two stages of the unload process, the lift point is offset towards the leading edge of the slider. This also causes a positive pitch and thus a "peeling" effect to reduce the lift-off force. The lift-off force dependence on

unload speed can be explained by the squeeze terms in the modified Reynolds equation that governs the air bearing.

VI. CONCLUSION

The dynamics of pico negative pressure sliders mounted on suspensions with flexure limitors were investigated during the unload process. New instrumentation was developed to measure the air bearing forces during dynamic L/UL. This instrumentation incorporates a high speed L/UL mechanism. Air bearing forces of a negative pressure slider were measured and simulated during the unload process. The following is a list of the important results.

1. The new experimental apparatus has good force transducer sensitivity and achieves a maximum vertical unload velocity of 15 mm/sec.

2. The unload force histories show a third stage associated with the limitors contacting the load beam. This contact causes the negative force to build up more rapidly than if the limitors were not present.

3. The force-displacement curve can be used to accurately determine the suspension parameters for use in the CML Dynamic L/UL software. Of these parameters, the lengthwise load point offset, X_d, is the most important for matching the simulation with the experimental data.

4. Knowledge of the force-displacement curve for a particular HGA design is crucial for suspension optimized for L/UL. The main concern here is the reduction of unload lift-off force and unload radial and vertical displacements.

5. As the disk rpm increases the lift-off force decreases.

6. As the unload speed increases the lift-off force increases.

7. To minimize the amount of dimple separation one should choose low unload speeds and high disk rpm.

ACKLOWLGEMENTS

REFERENCES

[1] Jeong, T. G., and Bogy, D. B., "An Experimental Study of the Parameters that Determine Slider-Disk Contacts During Dynamic Load-Unload," ASME J. of Tribology, Vol. 114, No. 3, pp. 507-514, 1992.

[2] Jeong, T. G., and Bogy, D. B., "Numerical Simulation of Dynamic Loading in Hard Disk Drives," ASME J. of Tribology, Vol. 115, No. 3, pp. 307-375, 1993.

[3] Fu, T. C., and Bogy, D. B., "Slider-Disk Contacts During the Loading Process in a Ramp-Load Magnetic Disk Drive," Adv. Info. Storage Syst., Vol. 6, pp. 41-54, 1995.

[4] Fu, T. C., and Bogy, D. B., "Drive Level Slider-Suspension Vibration Analysis and its Application to a Ramp-Load Magnetic Disk Drive," IEEE Tran. of Magnetics, Vol. 31, No. 6, pp. 3003-3005, 1995.

[5] Hu, Y., Jones, P. M., and Li, K., "Air Bearing Dynamics of Sub-Ambient Pressure Sliders During Dynamic Unload," ASME/STLE, International Tribology Conference, Toronto, Canada, Oct. 25-28, 1998.

[6] Peng, J. P., "Theoretical Prediction of Ramp Loading/Unloading Process in Hard Disk Drives," ASME/STLE, International Tribology Conference, Toronto, Canada, Oct. 25-28, 1998.

[7] Zeng , Q. H., Chapin, M., and Bogy, D. B., "Dynamics of the Unload Process for Negative Pressure Sliders," Asia-Pacific Magnetic Recording Conference, Singapore (APMRC), July 29-31, *IEEE Transaction of Magnetics* (in press).

[8] Zeng, Q. H., and Bogy, D. B., "The CML Dynamic Load/Unload Simulator," Technical Report No. 98-008, Computer Mechanics Lab., Dept. of Mechanical Engineering, Univ. of California at Berkeley, 1998.

[9] Albrecht, T., and Sai, F., "Load/unload Technology Finds Home in Mobile Drives," Data Storage, pp. 29-38, Sept., 1998.

Linear Slide

Servo Motor

Strain Arm

Cam Follower

HGA

Cam

Wire Coupling
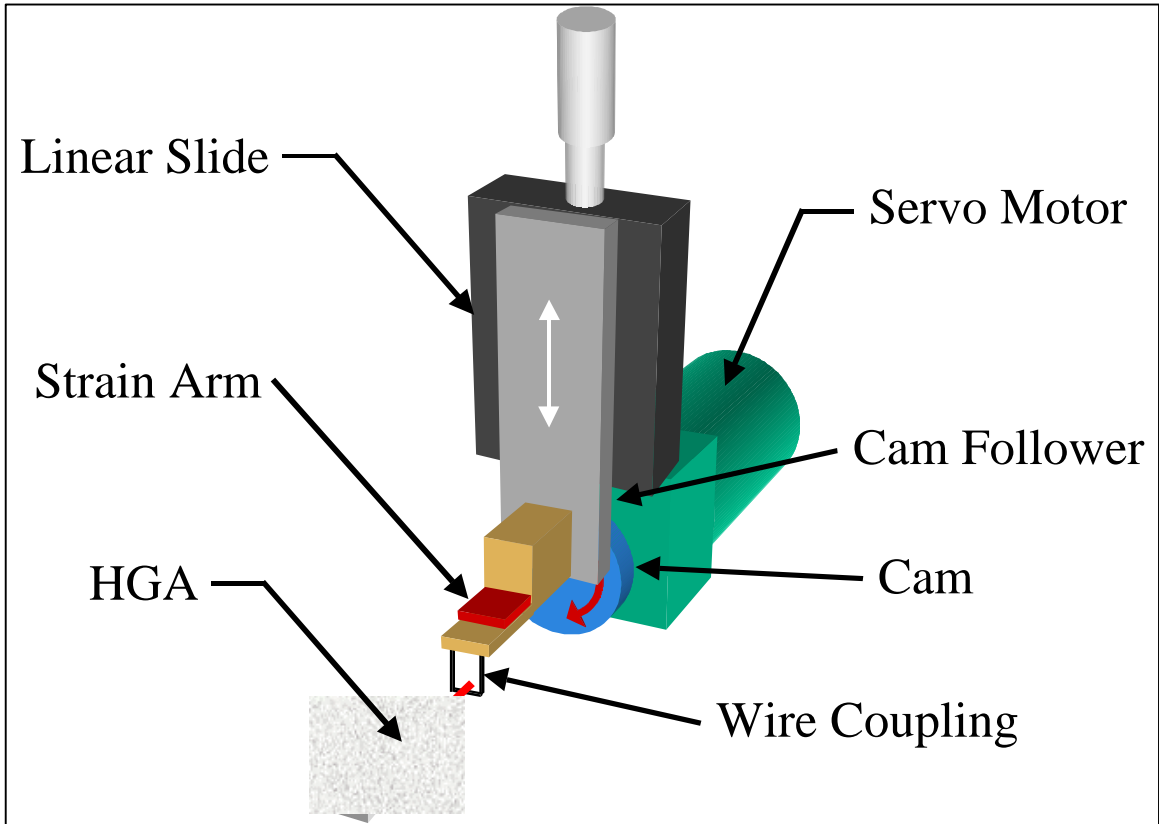
Figure 1: Cam driven vertical L/UL mechanism with strain arm force transducer
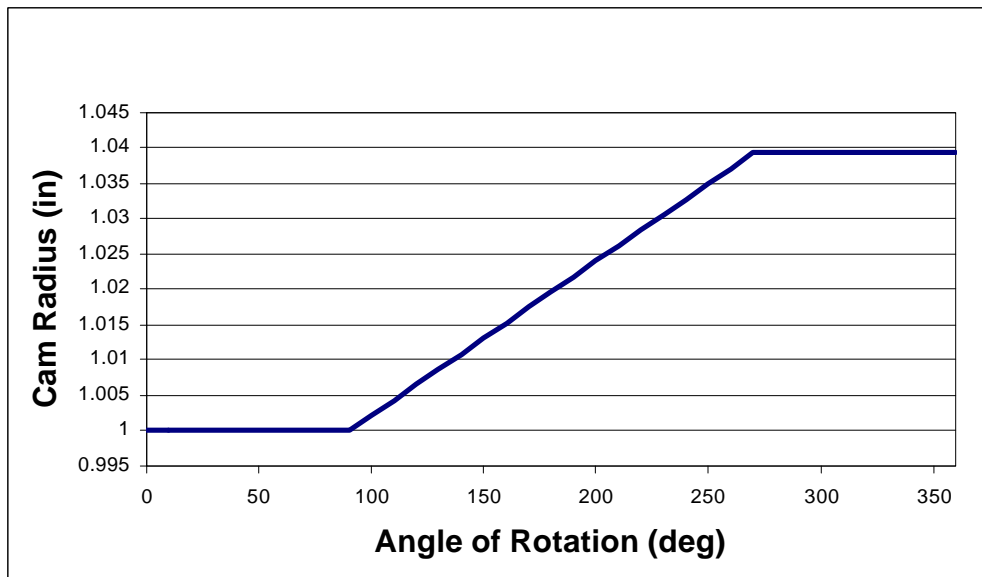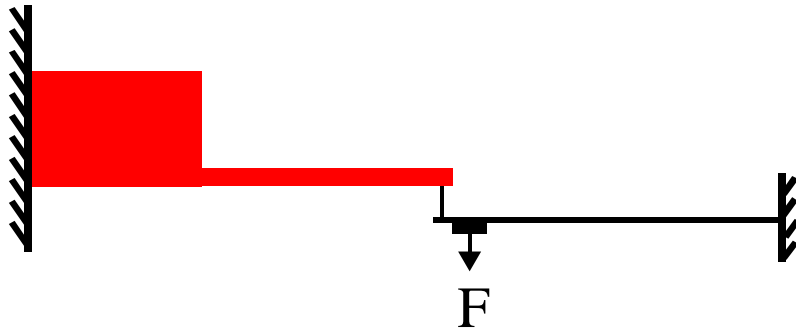
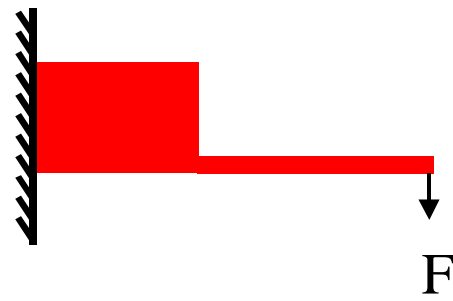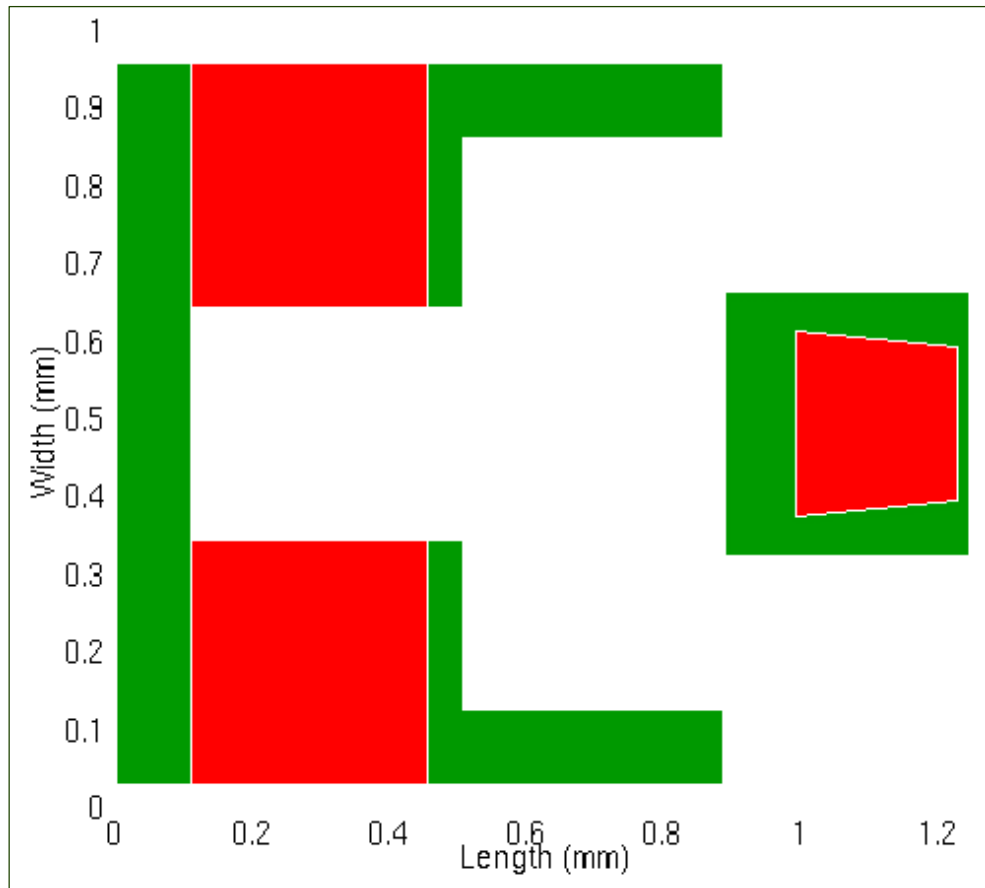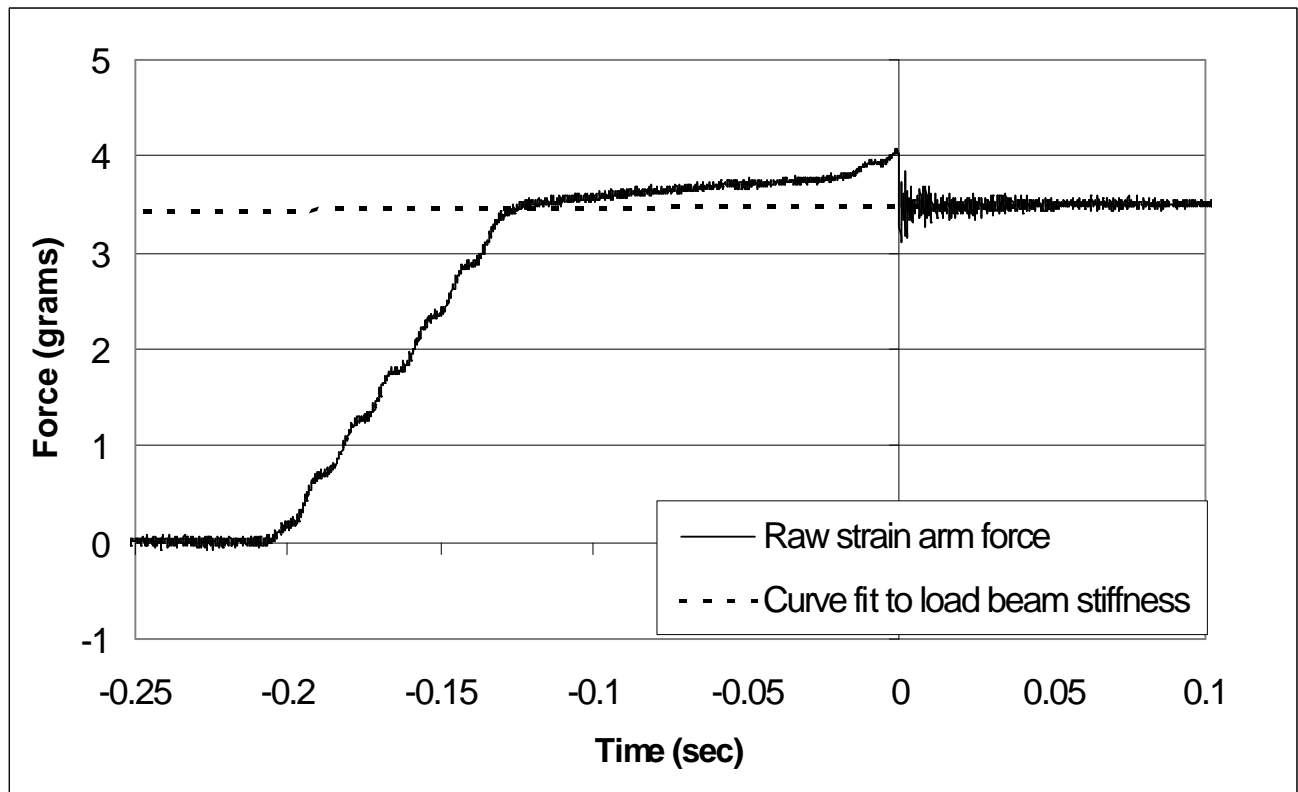**Figure 2: Radial profile of L/UL cam**
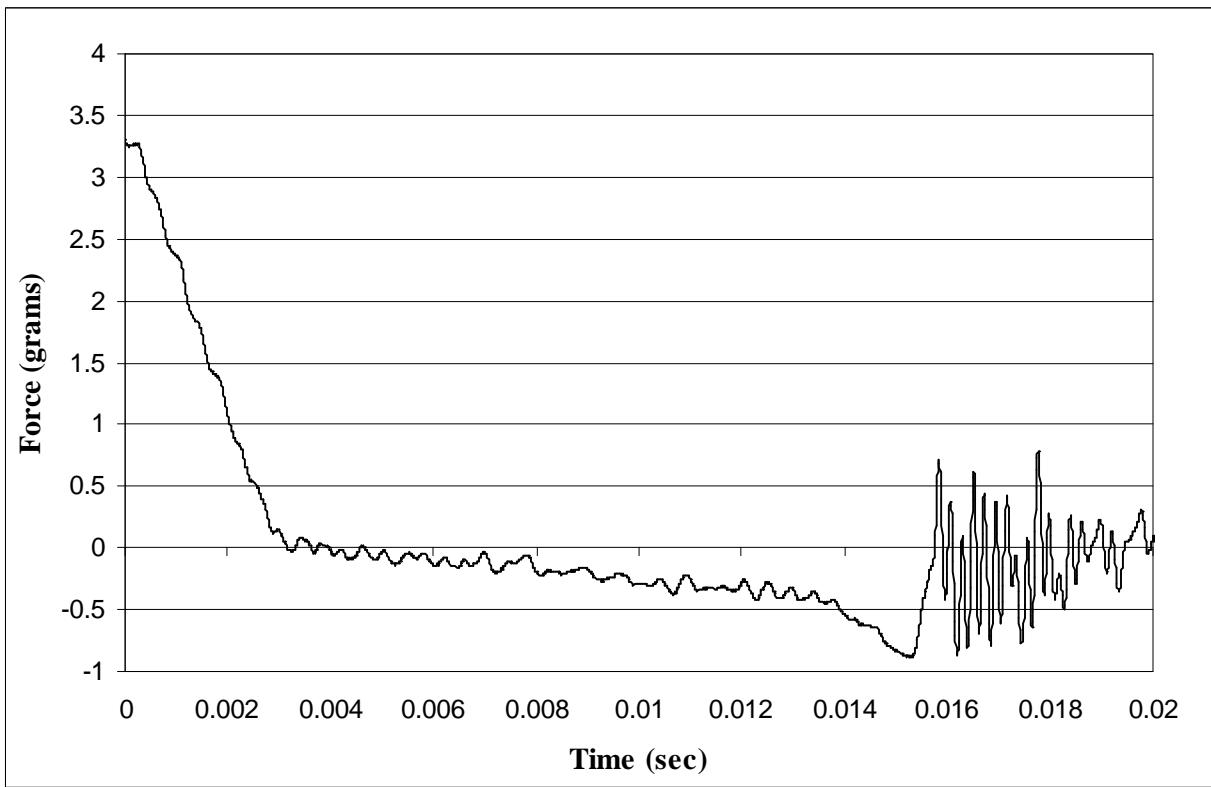
Figure 4(a)

Figure 4(b)

Figure 3: Two calibration methods (a) Calibration for forces located at the air bearing, (b) Calibration for forces located on the ramp
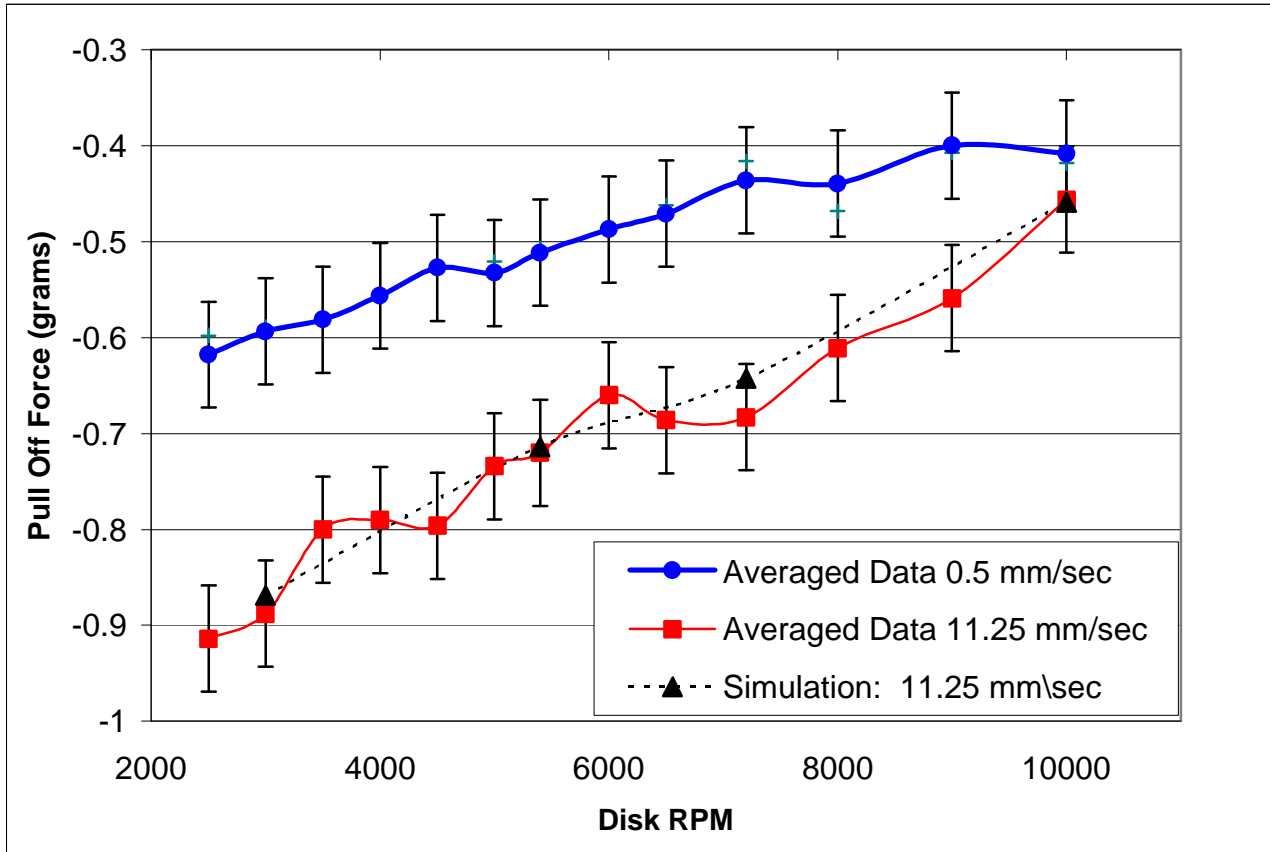
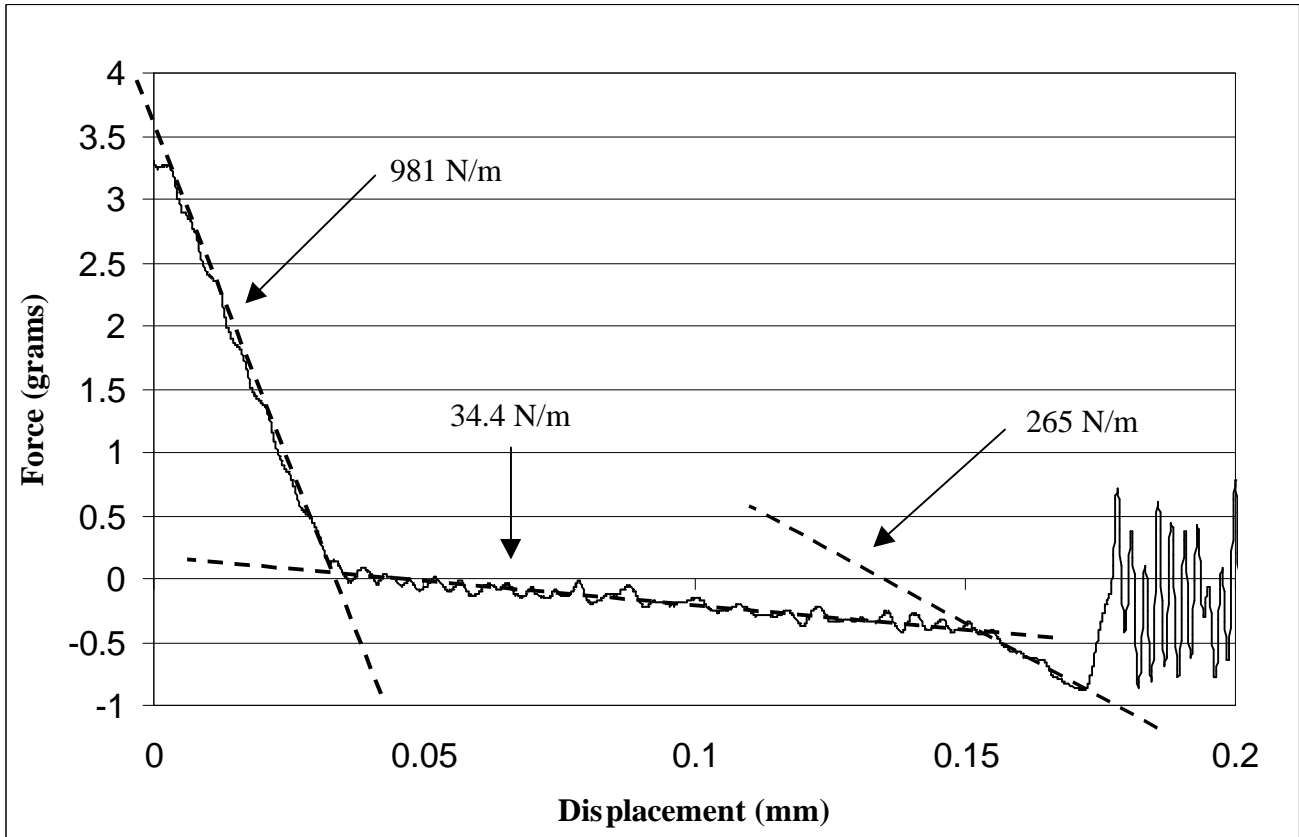**Figure 4: ABS design for the slider used in the study**

Figure 5: Raw force data for a typical unload process; 3000 rpm, 0.5 mm/sec unload speed

Figure 6: Processed unload force history at 3000 rpm and an unload speed of 11.25 mm/sec
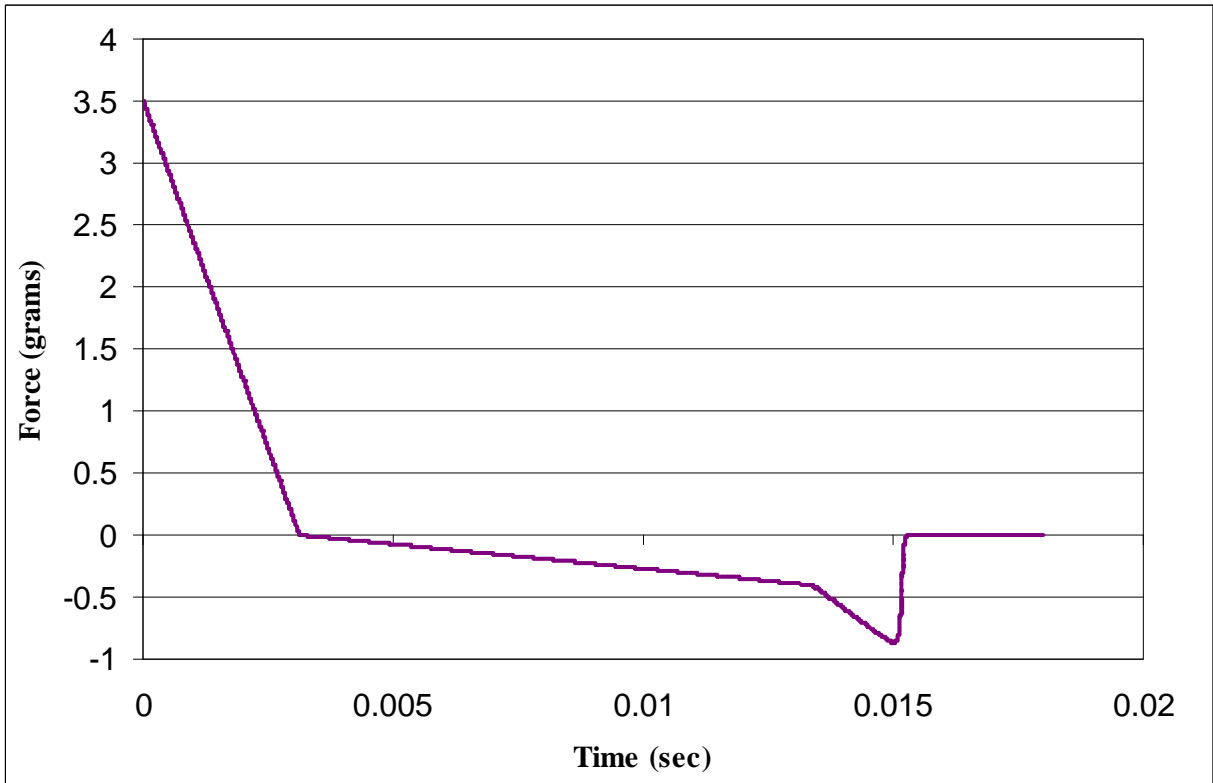
Figure 7: Dependence of lift-off-off force on disk rpm and unload velocity

Figure 8: Force-displacement curve, regional system stiffness shown

Figure 9: Simulated force history at 3000 rpm and an unload speed of 11.25 mm/sec